Viscoelasticity Effect on a Periodic Plane Medium Immersed in Water

Pierre Maréchal, Olivier Lenoir, Aissam Khaled, Mounsif Ech Cherif El Kettani, Driss Chenouni

Viscoelasticity Effect on a Periodic Plane Medium Immersed in Water

Pierre Maréchal[1)], Olivier Lenoir[1)], Aissam Khaled[2)], Mounsif Ech Cherif El Kettani[1)], Driss Chenouni[2)]

[1)] Laboratoire Ondes et Milieux Complexes (LOMC), UMR 6294 CNRS, Université du Havre, 75 rue Bellot, 76600 Le Havre, France. pierre.marechal@univ-lehavre.fr

[2)] Laboratoire d'Electronique, Signaux, Systèmes et d'Informatique (LESSI), Université Mohamed Ben Abdellah, Fès, Morocco

Summary

In this paper we are interested in the acoustic scattering by plane periodic media immersed in a fluid. In particular, the effects of viscosity on the stop and pass bands are investigated both theoretically and experimentally. We consider N periods of an elementary cell composed of two plates, presenting a high impedance contrast, with only one being considered viscous. Experimental results demonstrate the influence of the incidence side, and the developed theoretical models validate this phenomenon explicitly. A comparison of theoretical and experimental reflection spectra of a multilayered structure composed of N ($2 \leq N \leq 5$) periods of plane layers is presented in the frequency range from 0.5 to 3.5 MHz. The period consists of two isotropic plates considered as perfectly bonded, one in aluminum (elastic), the other in polyethylene (viscoelastic). Moreover, the influence of the number of periods is discussed. It is shown that the number of periods necessary to obtain stable stop and pass bands depends on the geometrical and physical characteristics of the viscoelastic plate. For the configurations under study, it is demonstrated that three periods ensure the convergence of the reflection spectrum.

PACS no. 43.20.El, 43.20.Gp, 43.20.Ks

1. Introduction

In literature, a number of works is reported dealing with elastic multilayered structure [1, 2, 3, 4, 5], presenting most of time, periodicity of elastic features. In this work, 1D phononic crystals (PC) are studied by their structure band properties useful for application is acoustic filtering [6] or vibration isolation [7] for instance. There are numerous theoretical methods to obtain the stop and pass bands of those PCs. Among them, the transfer matrix method (TMM) [8, 9, 10, 11, 12, 13], the finite-difference time-domain method (FDTD) [14, 15], and the plane-wave-expansion (PWE) [14, 16, 17]. Our theoretical approach is based upon the stiffness matrix method (SMM) [18, 19, 20, 21, 13] which ensures an unconditionnal numerical stability contrary to certain TMM. These methods allows us to study the stop and pass bands from the calculation of the reflection (R) and transmission (T) coefficients. Moreover, we take into account viscosity effects in the elementary period of the studied structure [22]. This one is asymmetric with respect to the median plane; it is composed on the one hand of an elastic plate and on the other hand of a viscoelastic one [23]. This lack of symmetry leads to differences between the calculated R coefficients according to the incidence side [24, 25]. To our knowledge the experimental and theoretical results presented here, dealing with those differences, have not been published. However, studies of stop and pass bands of such asymmetric periods have been performed in the (ω, k) plane [4]. In addition, we develop a new approach based on the Debye series method (DSM) [26, 27] which permits to highlight the finite number of viscoelastic stacks necessary to guarantee the stable frequency and amplitude characteristics of the R coefficients. Those theoretical aspects are validated experimentally.

The purpose of this study is to investigate the effect of viscosity on the reflection coefficients of a periodic plane multilayered structure composed of N periods ($2 \leq N \leq 5$). We are particularly interested in the influence of the insonification side on the scattering process of a periodic medium. It is shown that the pass and stop band shapes are affected. On one hand, the viscosity induces the damping of the resonance effects; on the other hand, the transmission coefficient is not strictly zero in the expected stop bands. In this work, the theoretical and experimental reflection spectra are compared for incidence angles varying between 0° and 30°. The elementary cell consists of two plates which are considered as perfectly bonded, one in aluminum, the other in polyethylene. The plates have the same thickness and exhibit a high acoustic impedance

Received 4 December 2013,
accepted 29 May 2014.

contrast, making it possible to establish well defined stop and pass bands. Viscosity is only taken into account in the polyethylene layer, for both longitudinal and transverse waves. Our study shows that the theoretical reflection coefficients differ according to the insonification side. These results are confirmed experimentally. In the second section, different theoretical models are described based on the Debye series expansion or transfer matrix method. Results at normal incidence are given in the third section. The reflected echoes are FFT processed and reflection spectra are deduced. These spectra are then compared to theoretical ones. In the fourth section, a study at oblique incidence is carried out for various angles of incidence. The locations of the minima of the experimental reflection spectra are compared to those of the reflection coefficients.

2. Theoretical models

The multilayered structure under study is assumed to be immersed in water. In this section, the theoretical expressions of the reflection and transmission coefficients at normal or oblique incidence are briefly recalled. Plots of these coefficients are compared with experimental results in sections 3 and 4. The geometry of the problem is given in Figure 1, showing multilayered structure immersed in water and insonified by an incident monochromatic plane wave with an incidence angle θ. Depending on the incidence side, the R_d (direct) reflection coefficient (resp. the R_r (reverse) reflection coefficient) is obtained when the wave impinges first the aluminum plate (resp. the polyethylene plate). To take into account the longitudinal and transverse waves attenuation in polyethylene, we consider a linear frequency dependent attenuation, which induces constant imaginary components δ_{c_L} and δ_{c_T} of the longitudinal and transverse wave velocities, respectively. We write the complex velocities in polyethylene as

$$\begin{aligned} c_L &= c_{L0}\left(1+\mathrm{j}\delta_{c_L}\right), \\ c_T &= c_{T0}\left(1+\mathrm{j}\delta_{c_T}\right), \end{aligned} \tag{1}$$

where $c_{L0,T0}$ are their real parts.

This results in a consistently admitted linear frequency dependence [28] of the imaginary part of the wave number $k_{L,T} \approx 2\pi f/c_{L0,T0} + \mathrm{j}\alpha_{L,T}$, i.e. the attenuation $\alpha_{L,T} = \alpha_{0,L,T} f$. The properties of the plates constituting the periodic structure are given in Table I. The uncertainty of the plate thickness is about 5%. The reflection coefficients can be obtained from a recursive procedure developed by Rokhlin *et al.* [20, 21], and are unconditionally stable, whatever the incidence angle θ. For N periods, the compliance matrix (4×4) is defined as

$$\mathbb{S}^N = \begin{bmatrix} S_{11}^N & S_{12}^N \\ S_{21}^N & S_{22}^N \end{bmatrix}. \tag{2}$$

The sub-matrices S_{ij}^N (2×2) for N periods are determined from the ones related to $(N-1)$ periods denoted as S_{ij}^{N-1},

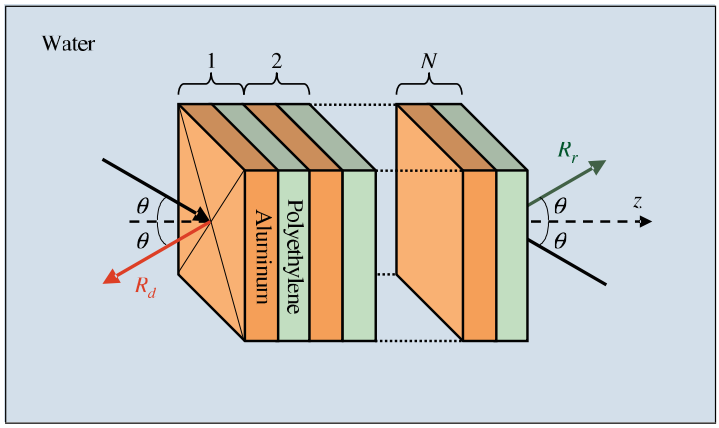

Figure 1. Geometry of the problem.

and the ones of a new period denoted as S_{ij} as

$$\begin{aligned} S_{11}^N &= S_{11}^{N-1} + S_{12}^{N-1}\left(S_{11} - S_{22}^{N-1}\right)^{-1} S_{21}^{N-1}, \\ S_{12}^N &= -S_{12}^{N-1}\left(S_{11} - S_{22}^{N-1}\right)^{-1} S_{21}, \\ S_{21}^N &= S_{21}\left(S_{11} - S_{22}^{N-1}\right)^{-1} S_{21}^{N-1}, \\ S_{22}^N &= S_{22} - S_{21}\left(S_{11} - S_{22}^{N-1}\right)^{-1} S_{12}. \end{aligned} \tag{3}$$

We show that the reflection coefficients $R_{d,r}$ (Figure 1) are expressed in terms of the (2,2) elements (exponents) of sub-matrices (indexes) $s_{ij} = S_{ij}^N(2,2)$ of the global compliance matrix $\boldsymbol{S}^N$ obtained for N periods [20, 21],

$$R_d = \frac{N_d}{D} = \frac{(s_{11}-y_F)(s_{22}-y_F)+(s_{12})^2}{(s_{11}+y_F)(s_{22}-y_F)+(s_{12})^2}, \tag{4}$$

$$R_r = \frac{N_r}{D} = \frac{(s_{11}+y_F)(s_{22}+y_F)+(s_{12})^2}{(s_{11}+y_F)(s_{22}-y_F)+(s_{12})^2}, \tag{5}$$

$$\text{and} \quad T = \frac{N_t}{D} = \frac{2y_F s_{12}}{(s_{11}+y_F)(s_{22}-y_F)+(s_{12})^2}, \tag{6}$$

where $y_F = \cos\theta/(\mathrm{j}\omega Z_F)$, with θ the angle of incidence, $Z_F = \rho_F c_F$ the acoustic impedance of the fluid, which is the product of its density ρ_F and its wave velocity c_F. Assuming real compliance matrices (i.e. lossless plates), it is numerically verified that the numerators are complex conjugates: $N_r = N_d^*$. Therefore, the modulus of the direct and reverse reflection coefficients are identical: $|R_d| = |R_r|$. Otherwise, those moduli are different [29]. Moreover, the transmission coefficient is independent of the incidence side. The energy conservation [28] can be written as

$$1 = \left|A_{d,r}\right|^2 + \left|R_{d,r}\right|^2 + \left|T\right|^2, \tag{7}$$

where the terms $A_{d,r}$ are the absorption coefficients, whose values depend on the incidence side. It is useful in the following to use a Debye series expansion to calculate these coefficients in the case of normal incidence [26, 27]. The multiple reflections at the interfaces between constitutive layers are considered recursively. At first, we define the Fresnel reflection and transmission coefficients at the interface between the layers numbered m and $m+1$,

$$\begin{aligned} R_{m,m+1} &= \frac{Z_{m+1}-Z_m}{Z_{m+1}+Z_m} \mathrm{e}^{\mathrm{j}\beta_m}, \\ T_{m,m+1} &= \frac{2Z_{m+1}}{Z_{m+1}+Z_m} \mathrm{e}^{-\mathrm{j}(\beta_{m+1}-\beta_m)}, \end{aligned} \tag{8a}$$

Table I. Acoustic properties of the layers. d: thickness; ρ: density; c_{L0}: longitudinal velocity; c_{T0}: transverse velocity; Z: acoustic impedance; δ_{c_L}: longitudinal losses; δ_{c_T}: transverse losses.

Medium	d (mm)	ρ (kg/m^3)	c_{L0} (m/s)	c_{T0} (m/s)	Z (MRa)	δ_{c_L} (%)	δ_{c_T} (%)
Al	4	2800	6380	3100	17.9	0	0
PE	4	940	2370	1200	2.22	1	10
H_2O	–	1000	1470	–	1.47	–	–

where $Z_m = \rho_m c_m$ is the acoustical impedance of layer m.

When the incidence is from the layers $(m+1)$ to the one m, the Fresnel coefficients are expressed as

$$R_{m+1,m} = \frac{Z_m - Z_{m+1}}{Z_m + Z_{m+1}} e^{-2j\beta_{m+1}},$$
$$T_{m,m+1} = \frac{2Z_m}{Z_{m+1} + Z_m} e^{-j(\beta_{m+1}-\beta_m)}, \quad (8b)$$

where $\beta_m = \omega z_m / c_{Lm}$ and $\beta_{m+1} = \omega z_m / c_{Lm+1}$ are phases which depend on the interface positions z_m, between the layers m and $m+1$.

As a result, the global reflection coefficient R at normal incidence is calculated recursively, from the layer M down to 1. This recursive approach ensures a numerical stability. The expression of the global reflection coefficient at normal incidence only is

$$R = R_{12} + \frac{T_{12}\rho_{23}T_{21}}{1 - R_{21}\rho_{23}}, \quad (9)$$

with

$$\rho_{m,m+1} = R_{m,m+1} + \frac{T_{m,m+1}\rho_{m+1,m+2}T_{m+1,m}}{1 - R_{m+1,m}\rho_{m+1,m+2}},$$

for $2 \leq m \leq M$ and $\rho_{M+1,M+2} = R_{M+1,M+2}$.

It is proved numerically that equations (4) and (5) are reduced to equation (9) in case of normal incidence.

3. Experimental study at normal incidence

3.1. Setup

The studied multilayered structure is immersed in a tank filled with water (Figure 2). The transducer used has a central frequency $f_0 = 2.25$ MHz, and it is excited by a pulse signal. At normal incidence, the transducer alternately acts as an emitter and as a receiver. The reflected response is acquired and averaged using a Yokogawa DL9240 oscilloscope linked with an Ethernet cable to a PC. The backscattered spectrum is obtained by performing the FFT of the whole response [30].

3.2. Reflection echoes

In Figure 3a, the two reflected signals according to the incidence side are compared. The amplitude of the first reflected echo (specular echo) is related to the acoustic properties of the first insonified plate. The following echoes correspond to the free resonant regime, due to multiple reflections within the multilayered structure. The longer

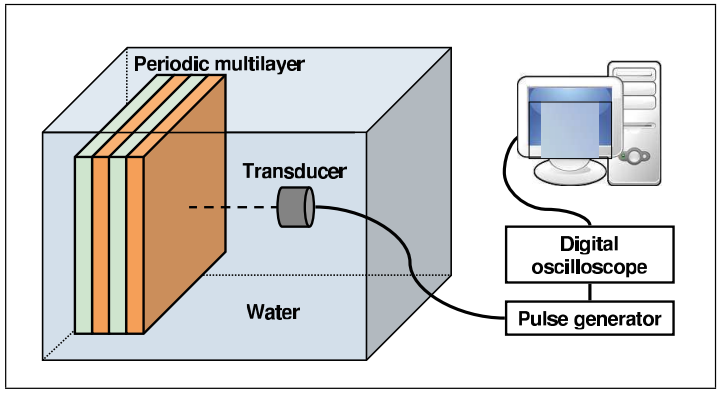

Figure 2. Experimental setup at normal incidence.

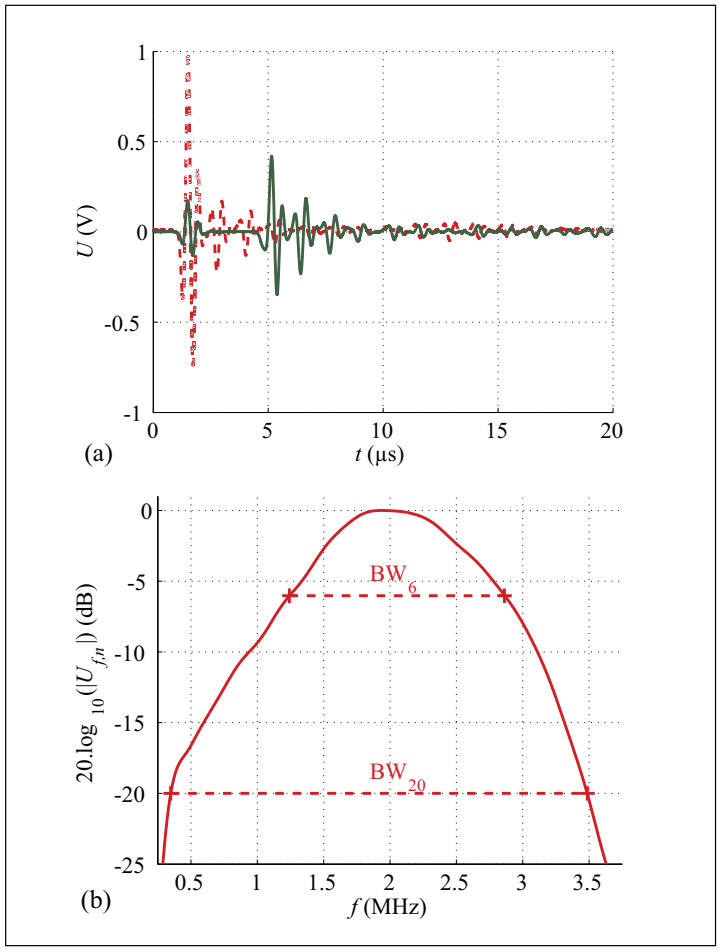

Figure 3. (a) Normalized amplitude of the echoes reflected at normal incidence, depending on the incidence side, either direct 5×(Al/PE) (dashed line) or reverse 5×(PE/Al) (solid line). (b) Spectrum of the specular echo and associated bandwidth.

the coda lasts, the more resonant is the response. In the signal reflected by the 5×(PE/Al) structure, we observe a specular echo on the polyethylene plate, a second on the aluminum plate, and echoes of multiple reflections. In the

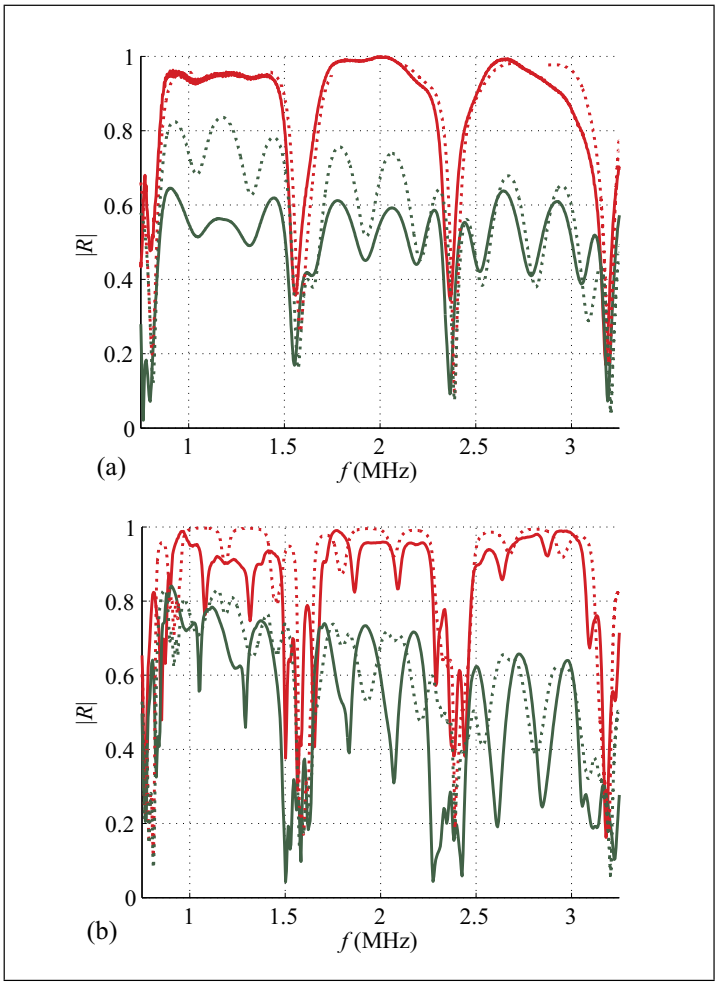

Figure 4. Reflection spectra $|R|$ theoretical (dotted) and experimental (solid) at normal incidence, depending on the incidence side, (a) direct (Al/PE) (two upper curves) or reverse (PE/Al) (two lower curves) and (b) direct 5×(Al/PE) (two upper curves) or reverse 5×(PE/Al) (two lower curves).

signal reflected by the 5×(Al/PE) structure, only a specular echo from the Al plate is clearly observed.

3.3. Reflection spectra

The reflection spectra are obtained by an FFT processing of the reflected signals. A pseudo- normalization is performed of each spectrum relative to its envelope. The reflection spectra are processed by taking into account the transducer's bandwidth centered at $f_c = 2\,\text{MHz}$. In Figure 3b, the measured relative bandwidths have the values at half maximum, $BW_6/f_c = 78\%$ and at $-20\,\text{dB}$, $BW_{20}/f_c = 164\%$. They ensure the accurate measurement of the reflection coefficient over a wide frequency domain ranging from 750 kHz to 3.25 MHz. In accordance with the theory, the experimental reflection spectra depend on the incidence side, either direct $N\times$(Al/PE) or reverse $N\times$(PE/Al) (Figure 4, (a) $N = 1$, (b) $N = 5$). The difference of the spectra between direct or reverse incidence is explained by the fact that the PE plate is lossy. Attenuation, at the frequency around 2 MHz, is not negligible in polyethylene and must be considered. In the reflection spectra shown in Figure 4a, there are marked minima associated with resonances due to the thickness modes of the aluminum plate. These minima are separated by the frequency interval $\Delta f_{\text{Al}} = c_{L,\text{Al}}/(2d_{\text{Al}}) \approx 800\,\text{kHz}$. The other local minima correspond to resonances due to the thickness modes of the polyethylene plate, and separated by $\Delta f_{\text{PE}} \approx 300\,\text{kHz}$ [29]. As shown in Figure 4, the positions of the marked local minima obtained experimentally are close to theoretical ones. Nevertheless, the uncertainties in the thickness of the multiple plates in the manufactured structures cause problems because a strict periodicity is considered in theory. For example in Figure 4b, some minima mismatch in location as well as in amplitude. In the case of an elementary (Al/PE) cell, the reflection coefficient (equation 9) can be expressed as

$$R = R_{12}\left(1 + TR_{1221}\frac{K}{1-K}\right), \tag{10}$$

$$\text{where} \quad K = RR_{2123}\left(1 + TR_{2332}\frac{RR_{3234}}{1-RR_{3234}}\right). \tag{11}$$

In the following by considering either the direct (indexed d) or reverse (indexed r) insonification, the direct R_d or reverse R_r reflection coefficients, as well as the respective direct K_d or reverse K_r coefficients are obtained from equations (10) and (11) giving the general expressions for R and K.

These coefficients (equations 10 and 11) are expressed as functions of the products of the Fresnel reflection and transmission coefficients (equations 8 and 9),

$$TR_{m,m+1,m+1,m} = \frac{T_{m,m+1}T_{m+1,m}}{R_{m,m+1}R_{m+1,m}} = \frac{-4Z_mZ_{m+1}}{(Z_m - Z_{m+1})^2} \tag{12}$$

and

$$\begin{aligned} RR_{m,m-1,m,m+1} &= R_{m,m-1}R_{m,m+1} = rr_{m,m-1,m,m+1}\mathrm{e}^{+\mathrm{j}2k_md_m} \\ &= \frac{(Z_{m-1} - Z_m)(Z_{m+1} - Z_m)}{(Z_{m-1} + Z_m)(Z_{m+1} + Z_m)}\mathrm{e}^{+\mathrm{j}2k_md_m}. \end{aligned} \tag{13}$$

As highlighted by equation (13), the following decomposition of the phase $\mathrm{j}2k_md_m = -\alpha_md_m + \mathrm{j}2\pi f/\Delta f_m$ associated with the layer m reveals a real component related to the attenuation α_m and an imaginary component involving the frequency periodicity $\Delta f_m = c_{Lm}/(2d_m)$. So, the direct K_d or reverse K_r coefficients, as well as the respective direct R_d or reverse R_r reflection coefficients are expressed as

$$\begin{aligned} K_d = {} & rr_{2123}\mathrm{e}^{+\mathrm{j}2\pi f/\Delta f_{\text{Al}}} \\ & \cdot\left(1 + TR_{2332}\frac{rr_{3234}\mathrm{e}^{-2\alpha_{\text{PE}}d_{\text{PE}}}\mathrm{e}^{+\mathrm{j}2\pi f/\Delta f_{\text{PE}}}}{1 - rr_{3234}\mathrm{e}^{-2\alpha_{\text{PE}}d_{\text{PE}}}\mathrm{e}^{+\mathrm{j}2\pi f/\Delta f_{\text{PE}}}}\right) \end{aligned} \tag{14}$$

and

$$\begin{aligned} K_r = {} & rr_{2123}\mathrm{e}^{-2\alpha_{\text{PE}}d_{\text{PE}}}\mathrm{e}^{+\mathrm{j}2\pi f/\Delta f_{\text{Al}}} \\ & \cdot\left(1 + TR_{2332}\frac{rr_{3234}\mathrm{e}^{+\mathrm{j}2\pi f/\Delta f_{\text{Al}}}}{1 - rr_{3234}\mathrm{e}^{+\mathrm{j}2\pi f/\Delta f_{\text{Al}}}}\right). \end{aligned} \tag{15}$$

These plots of the K_d or K_r coefficients exhibit local minima (Figure 5) separated either by the period Δf_{PE} or Δf_{Al}, respectively. As a result, the mean values of the multiple reflection coefficients are $|K_d|_{rm,mean} \approx 0.66$ and $|K_r|_{,\text{mean}} \approx 0.10$, for the direct and reverse incidence side.

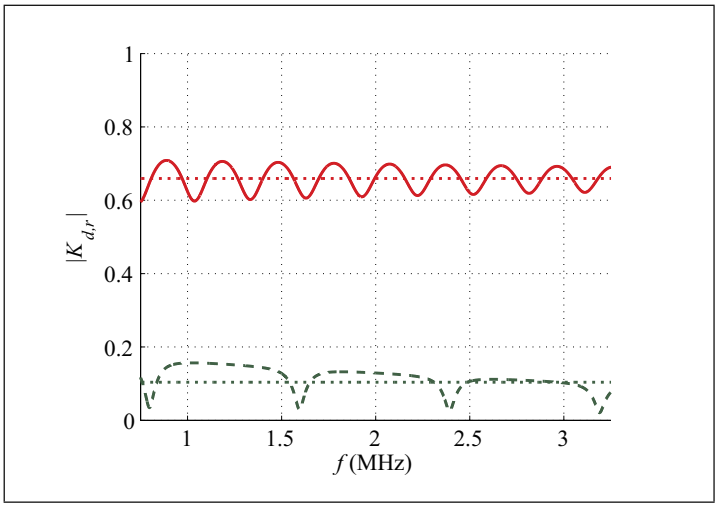

Figure 5. Multiple reflection coefficients $|K_d|$ and $|K_r|$, depending on the incidence side, direct (Al/PE) (solid) or reverse (PE/Al) (dashed).

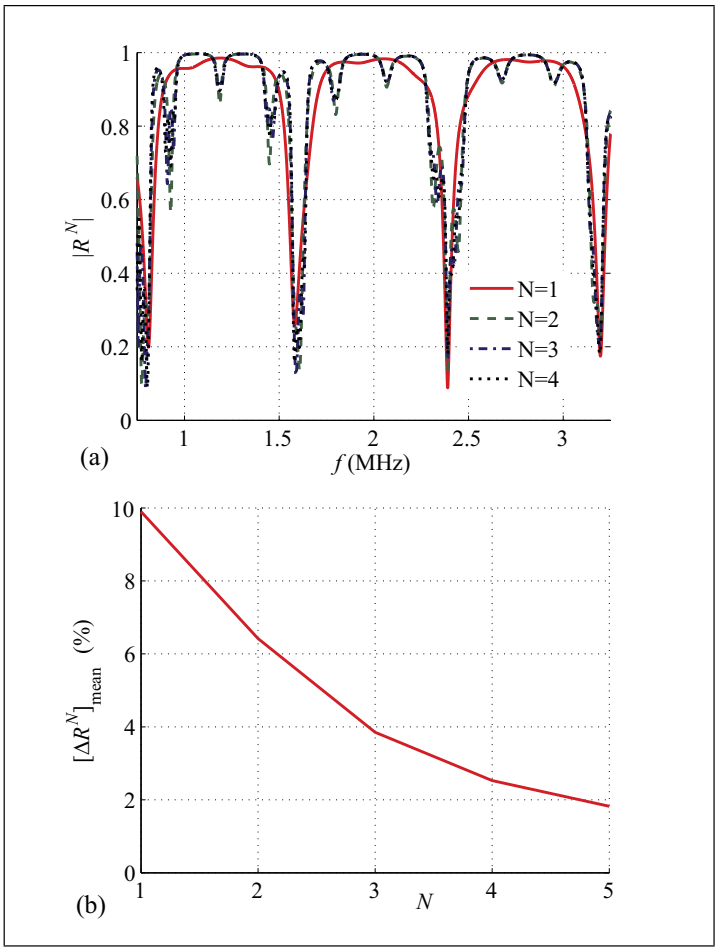

Figure 6. Theoretical (a) direct reflection spectra $|R^N|$ for $N\times$(Al/PE) and (b) associated mean relative difference $[\Delta R^N]_{\text{mean}} = [||R^N| - |R^{N-1}||/|R^{N-1}|]_{\text{mean}}$ between the $N\times$(Al/PE) and the $(N-1)\times$(Al/PE) configurations.

Thus a small $|K|$ value leads to a reflection coefficient R approaching R_{12} (equation 10). This demonstration can be generalized to the case of N periods, showing a rapid convergence. It can be seen in Figure 6a, that beyond $N = 3$ periods, there is no more significant change of the reflection spectra. In order to quantify this phenomenon we introduce a relative difference of two successive moduli of

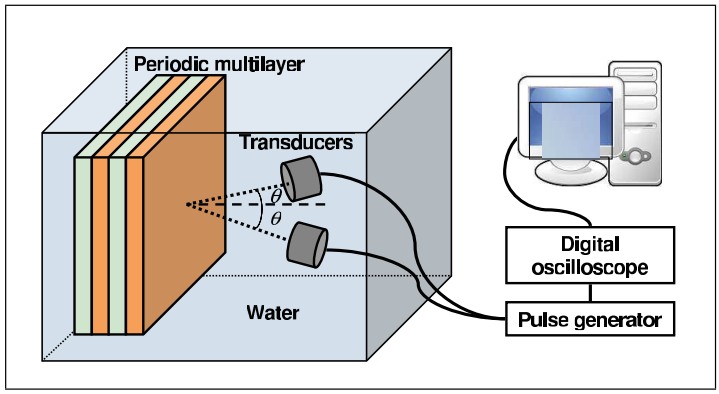

Figure 7. Experimental setup at oblique incidence.

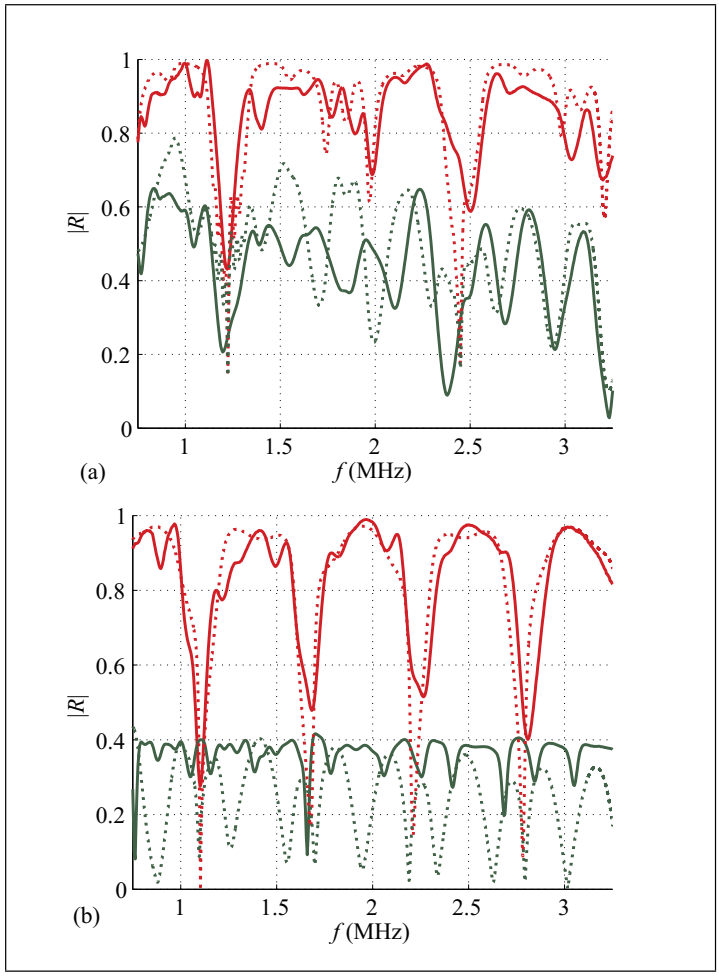

Figure 8. Reflection spectra $|R|$ theoretical (dotted line) and experimental (continuous) depending on the insonification side, direct $5\times$(Al/PE) (two upper curves) or reverse $5\times$(PE/Al) (two lower curves), oblique incidence a) $\theta = 10°$, b) $\theta = 20°$.

reflection coefficients as

$$\left[\Delta R^N\right]_{\text{mean}} = \frac{1}{f_{\max} - f_{\min}} \int_{f_{\min}}^{f_{\max}} \frac{\left||R^N| - |R^{N-1}|\right|}{|R^{N-1}|} \mathrm{d}f, \quad (16)$$

where $[f_{\min}; f_{\max}] = [0.75; 3.25]$ MHz and $N > 1$.

Figure 6b presents the plot of $[\Delta R^N]_{\text{mean}}$; we can observe that $[\Delta R^3]_{\text{mean}}$ is less than 4%. It is thus shown that attenuation plays an important role in the reflective properties of a periodic structure.

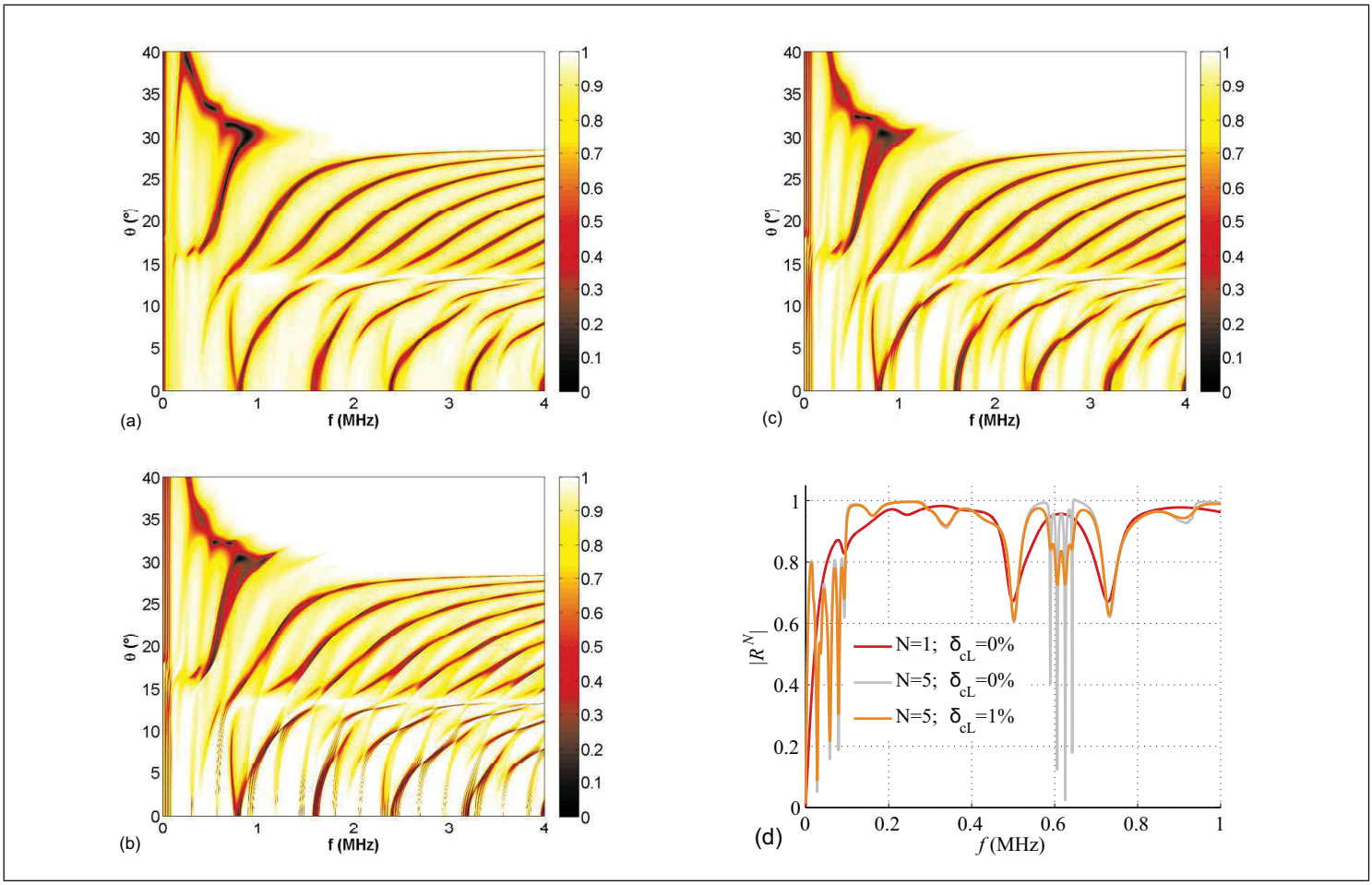

Figure 9. Theoretical dispersion curves with $\delta_{cT} = 10\%$ in the (a) (Al/PE) longitudinal lossless structure, (b) 5×(Al/PE) longitudinal lossless structure, (c) 5×(Al/PE) longitudinal lossy structure with $\delta_{cL} = 1\%$, (d) cut at $\theta = 10°$ for the (a), (b), (c) configurations.

4. Experimental study at oblique incidence

Two transducers are used, one in emission, the other in reception (Figure 7). They are oriented at the same angle θ with respect to the normal of the structure, which is varied from 0 to 40° by steps of 5°. The electronic setup and signal processing are the same as in the case of normal incidence. The reflection coefficients for a 5 period multilayered structure are plotted for $\theta = 10°$ in Figure 8a and $\theta = 20°$ in Figure 8b. There is a significant difference between the plots of the reflection coefficients according to the incidence side. This difference increases with the incidence angle. The agreement between the experimental and theoretical minima is good in the case of the 5×(Al/PE) structure for all incidence angles. For the 5×(PE/Al) structure, this agreement is good only at high frequencies above 2.5 MHz. The modulus of the direct reflection coefficient $|R|$ in the frequency/incidence angle plane gives a good overview of the dispersion curves [31, 32] of modes propagating in the lossless (Al/PE) and 5×(Al/PE) structures, illustrated by Figure 9a and 9b, respectively. The lines connecting reflection zeroes in the frequency/incidence angle plane $|R(f, \theta)| = 0$ are assimilated to dispersion curves. It is to be noted that these dispersion curves are very close to the ones of an aluminum plate. We observe (Figure 9b) the multiplication of curves compared to the case of a single cell (Figure 9a). An N period multilayer structure implies $(N - 1)$ curves at very low frequency associated with the

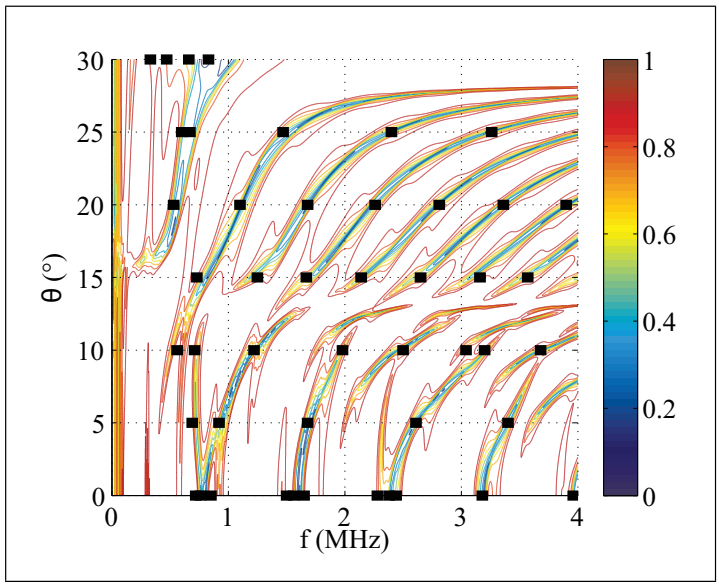

Figure 10. Superimposition of the experimental minima and the theoretical dispersion curves obtained for a 5×(Al/PE) lossy structure, with $\delta_{cL} = 1\%$ and $\delta_{cT} = 10\%$.

so-called vertical modes [3, 4, 5]. Similarly, at high frequency, N dispersion curves are observed in the vicinity of the ones of a single cell. As illustrated in Figure 9a, 9b and 9c, one can identify with plateaus the longitudinal and transverse critical angles of refraction related to aluminum ($\theta_{L,\mathrm{Al}} = 13.4°$, $\theta_{T,\mathrm{Al}} = 28.5°$, respectively). Beyond the longitudinal critical angle associated with polyethylene

($\theta_{L,\mathrm{PE}} = 38.6°$), for $f > 1\,\mathrm{MHz}$, the reflection is total. As illustrated by the thin dispersion curves for the lossless case (Figure 9b), the resonances observed are very narrow. In the case where losses are taken into account (Figure 9c), the general shape of the dispersion curves remains the same, but those which are close have "merged" into a single broad one (the associated resonances are also broadened). This is a direct effect of the losses. A more systematic comparison of the minima of the reflection spectra as a function of incidence angle (Figure 10) shows a good agreement between experimental and theoretical results (Figure 9c). Indeed, the differences between experiment and theory are explained partly by the uncertainties in the thicknesses of the plates constituting the multilayer structure, which involve variations in frequency with an estimated shift $\Delta f \approx \pm 50\,\mathrm{kHz}$ on the one hand, and by the uncertainty $\Delta\theta \approx \pm 0.5°$ on the angular position on the other hand. Experimental results show the importance of the characterization of viscoelastic material properties used for the multilayered structure. Indeed, the attenuation in the polyethylene plate α_{PE} has a strong influence on the reflection coefficient R (equation 10) through the coefficients $K_{d,r}$ (equations 14 and 15) which significantly alters the expected dispersion curves. The other source of alteration is the uncertainties in the plate thicknesses which are around 5%.

5. Conclusion

In this study, the reflective properties of a multilayered structure depending on the insonification side are highlighted. The viscoelastic properties of materials such as polyethylene are taken into account to explain the observed physical phenomena. It is shown experimentally and verified theoretically that the losses have a significant influence, both in terms of amplitude and position of the minima of reflection. In our case, the comparison between experimental and theoretical results is good. Further study will consist in taking into account uncertainties in viscoelastic plate thicknesses and bonding with glue films between plates and periods.

Acknowledgement

The authors thank H. Cahingt for the realization of multilayer assemblies, F. Duhamel for the experimental part and D. Hallidy for her english rereading.

References

[1] D. Folds, C. Loggins: Transmission of acoustic waves in layered media. Journal of the Acoustical Society of America **62** (1977) 1102–1109.

[2] M. Rousseau: Floquet wave properties in a periodically layered medium. Journal of the Acoustical Society of America **86** (1989) 2369–2376.

[3] P. Gatignol, J. Moukemaha: Polynômes de Tchebytchev et modes de transmission totale dans les multicouches périodiques. Proc. Third French Conf. on Acoust., J. Phys. IV **C5** (1994) 817–820.

[4] P. Gatignol, C. Potel, J. DeBelleval: Two families of modal waves for periodic structures with two field functions: A Cayleigh-Hamilton approach. Acta Acustica united with Acustica **93** (2007) 959–975.

[5] A. Khaled, P. Maréchal, O. Lenoir, M. E.-C. El-Kettani, D. Chenouni: Study of the resonances of periodic plane media immersed in water: Theory and experiment. Ultrasonics **53** (2013) 642–647.

[6] I. K. Lee, Y. J. Kim, J. H. Oh, Y. Y. Kim: One-dimensional broadband phononic crystal filter with unit cells made of two non-uniform impedance-mirrored elements. AIP Advances **3** (2013) 1–9.

[7] C.-Y. Lee, M. J. Leamy, J. H. Nadler: Frequency band structure and absorption predictions for multi-periodic acoustic composites. Journal of Sound and Vibration **329** (2010) 1809–1822.

[8] M. Zheng, P. J. Wei: Band gaps of elastic waves in 1-D phononic crystals with imperfect interfaces. International Journal of Minerals, Metallurgy and Materials, **16** (2009) 608–614.

[9] F. Kobayashi, S. Biwa, N. Ohno: Wave transmission characteristics in periodic media of finite length: multilayers and fiber arrays. International Journal of Solids and Structures **41** (2004) 7361–7375.

[10] M. I. Hussein, G. M. Hulbert, R. A. Scott: Dispersive elastodynamics of 1D banded materials and structures: Design. Journal of Sound and Vibration **307** (2007) 865–893.

[11] M. I. Hussein, G. M. Hulbert, R. A. Scott: Dispersive elastodynamics of 1D banded materials and structures: Analysis. Journal of Sound and Vibration **289** (2006) 779–806.

[12] A.-L. Chen, Y.-S. Wang: Study on band gaps of elastic waves propagating in one-dimensional disordered phononic crystals. Physica B: Condensed Matter **392** (2007) 369–378.

[13] E. L. Tan: Generalized eigenproblem of hybrid matrix for Floquet wave propagation in one-dimensional phononic crystals with solids and fluids. Ultrasonics **50** (2010) 91–98.

[14] P. Nowak, M. Krawczyk: Phononic band gaps in one-dimensional phononic crystals with nanoscale periodic corrugations at interfaces. FDTD and PWM simulations. Computational Methods in Science and Technology **16** (2010) 85–95.

[15] P.-F. Hsieh, W. Tsung-Tsong, S. Jia-Hong: Three-dimensional phononic band gap calculations using the FDTD method and a PC cluster system. IEEE Ultrasonics, Ferroelectrics and Frequency Control Society **53** (2006) 148–158.

[16] G. Wang, D. Yu, J. Wen, Y. Liu, X. Wen: One-dimensional phononic crystals with locally resonant structures. Physics Letters A **327** (2004) 512–521.

[17] Y. Zhao, P. Wei: The band gap of 1D viscoelastic phononic crystal. Computational Materials Science **46** (2009) 603–606.

[18] B. Hosten: Bulk heterogeneous plane waves propagation through viscoelastic plates and stratified media with large values of frequency domain. Ultrasonics **29** (1991) 445–450.

[19] B. Hosten, M. Castaings: Surface impedance matrices to model the propagation in multilayered media. Ultrasonics **41** (2003) 501–507.

[20] L. Wang, S. Rokhlin: Stable reformulation of transfer matrix method for wave propagation in layered anisotropic media. Ultrasonics **39** (2001) 413–424.

[21] S. Rokhlin, L. Wang: Stable recursive algorithm for elastic wave propagation in layered anisotropic media: Stiffness

matrix method. Journal of the Acoustical Society of America **112** (2002) 822–834.

[22] H. Zhao, Y. Liu, D. Yu, G. Wang, J. Wen, X. Wen: Absorptive properties of three-dimensional phononic crystal. Journal of Sound and Vibration **303** (2007) 185–194.

[23] H. C. Strifors, G. C. Gaunaurd: Selective reflectivity of viscoelastically coated plates in water. The Journal of the Acoustical Society of America **88** (990) 901–910.

[24] B. Mace: Reciprocity, conservation of energy and some properties of reflection and transmission coefficients. Journal of Sound Vibration **155** (1992) 375–381.

[25] A. Maznev, A. Every, O. Wright: Reciprocity in reflection and transmission: What is a phonon diode? Wave Motion **50** (2013) 776–784.

[26] J. Conoir: Réflexion et tra nsmission par une plaque fluide. La diffusion acoustique. Chap. 5. P. Cedocar, N. Gespa, ISBN 2717008845 (1987) 105–132.

[27] P. Maréchal, L. Haumesser, L. Tran-Huu-Hue, J. Holc, D. Kuscer, M. Lethiecq, G. Feuillard: Modeling of a high frequency ultrasonic transducer using periodic structures. Ultrasonics **48** (2008) 141–149.

[28] R. Fiorito, W. Madigosky, H. Überall: Theory of ultrasonic resonances in a viscoelastic layer. Journal of the Acoustical Society of America **77** (1985) 489–498.

[29] O. Lenoir, P. Maréchal: Study of plane periodic multilayered viscoelastic media: Experiment and simulation. IEEE International Ultrasonics Symposium Proceedings, 2009, 1028–1031.

[30] S. Derible, F. Coulouvrat, M. Rousseau, J. Izbicki, T. A.: Analysis of a sandwich elastic plate structure by means of its transition terms. Proceedings of the Acoustics 2012 Nantes Conference, 35, Nantes, 2012, 509–515.

[31] O. Lenoir, J. Izbicki, M. Rousseau, F. Coulouvrat: Subwavelength ultrasonic measurement of a very thin fluid layer thickness in a trilayer. Ultrasonics **35** (1997) 509–515.

[32] F. Coulouvrat, M. Rousseau, O. Lenoir, J. Izbicki: Lamb-type waves in symmetric solid-fluid-solid trilayer. Acta Acustica **84** (1998) 12–20.